Non-Stationary Interference Cancellation in HF Surface Wave Radar

Giuseppe A. Fabrizio*, Alex B. Gershman†, Mike D. Turley*
* Radar Signal Processing Group, Intelligence Surveillance and Reconnaissance Division,
Defence Science and Technology Organisation, Edinburgh, SA, 5111, Australia.
Email: joe.fabrizio@dsto.defence.gov.au, mike.turley@dsto.defence.gov.au
† Communications Research Laboratory, Department of Electrical and Computer Engineering,
McMaster University, 1280 Main St W., Hamilton, Ontario, Canada L8S 4K1.
Email: gershman@ieee.org

***Abstract*— High frequency (HF) interference in surface wave over-the-horizon (OTH) radars typically exhibits a time-varying or non-stationary spatial structure. Adaptive beamformers that update the spatial filtering weight vector *within* the coherent processing interval (CPI) are likely to suppress such interference most effectively, but the intra-CPI antenna pattern fluctuations result in temporal de-correlation of the clutter which severely degrades sub-clutter visibility after Doppler processing. A robust adaptive beamformer that effectively suppresses non-stationary interference without degrading sub-clutter visibility is proposed. The new algorithm is computationally efficient and suitable for practical implementation. Its operational performance is evaluated using experimental data recorded by the Iluka HF surface wave (HFSW) OTH radar, located near Darwin in far north Australia.**

I. Introduction

HFSW radars operate by normal line-of-sight propagation in addition to surface wave propagation [1]. The latter enables surface and airborne targets to be detected at ranges of up to 200-300 kilometres over sea water [2], [3]. Offshore targets of emerging interest include "sea-skimming" missiles [4], and small "go-fast" boats used for smuggling and drug trafficking [5], [6]. Doppler processing can usually resolve high velocity targets from the most powerful (first-order) ocean clutter returns. This often allows fast-moving targets with small radar cross section (RCS) to compete for detection against interference-plus-noise.

In the user-congested HF spectrum, unoccupied frequency channels of sufficient bandwidth (50-100 kHz) are at times extremely difficult to find, particularly in the lower HF band (5-15 MHz) or at night time when the ionosphere is known to propagate interference sources very long distances. The ionospheric or skywave propagation is detrimental to HFSW radar because it effectively increases the number of interferers at the radar site, making it sometimes impossible to find a "silent" frequency channel to operate the radar [7], [8]. In such situations, the signal-to-interference plus noise ratio (SINR) can be enhanced by using adaptive beamforming to cancel directional interference from natural and man-made sources.

Radio frequency interference (RFI) typically exhibits a *time-varying* spatial structure statistically characterised by a non-stationary spatial covariance matrix over the CPI. This physical phenomenon may arise due to the dynamic properties of the ionospheric layer(s) propagating interference [9], the variation in geometry between radar receiver and interference source(s) [10], or the impulsive nature of the source(s) [11]. Experimental investigations confirm that RFI spatial non-stationarity *within* typical OTH radar CPI has a pronounced impact on adaptive beamformer performance and must be taken into accounted to ensure effective HF interference suppression, see [9], [12] for example. The long dwell times required by HFSW radars (CPIs of 30-120 seconds) means that standard adaptive beamforming implementations based on *time-invariant* array weight vectors often fail to significantly improve the SINR. For this reason, such systems are highly susceptible to the RFI spatial non-stationarity phenomenon.

The alternative is to update the adaptive beamforming weights within the CPI. Time-varying weights are likely to yield more effective interference cancellation while providing distortionless (unity gain) response to target signals incident from the radar look direction, but the beamformed clutter component may suffer a severe loss of temporal coherence as it is received over the *entire* adaptive antenna pattern which (for non-stationary interference) may be required to *fluctuate* during the CPI. This degradation manifests itself as a smearing of the clutter energy across the Doppler (velocity) search space with the potential to obscure the presence of useful signals.

We propose a robust adaptive beamformer that effectively suppresses non-stationary interference without significantly degrading sub-clutter visibility. A desirable property of the algorithm is that its computational cost is much lower than the *Stochastic Constraints* (SC) method previously used to address this problem [14]. Apart from its computational efficiency, the new method is also more robust to estimation errors that can accumulate with each update and degrade Doppler processing performance. Both qualities make it an attractive candidate for practical implementation in operational HFSW radar systems. The array data model is described in section 2. Section 3 describes the proposed algorithm. Section 4 presents and discusses the experimental results that compare the performance of the proposed algorithm with the conventional beamformer, the sample matrix inverse (SMI) technique and the SC method. Conclusions are given in section 5.

0-7803-7871-7/03/$17.00 © 2003 IEEE

Report Documentation Page

Form Approved
OMB No. 0704-0188

1. REPORT DATE	2. REPORT TYPE	3. DATES COVERED
14 APR 2005	**N/A**	**-**

4. TITLE AND SUBTITLE	5a. CONTRACT NUMBER
Non-Stationary Interference Cancellation in HF Surface Wave Radar	5b. GRANT NUMBER
	5c. PROGRAM ELEMENT NUMBER
6. AUTHOR(S)	5d. PROJECT NUMBER
	5e. TASK NUMBER
	5f. WORK UNIT NUMBER
7. PERFORMING ORGANIZATION NAME(S) AND ADDRESS(ES) **Radar Signal Processing Group, Intelligence Surveillance and Reconnaissance Division, Defence Science and Technology Organisation, Edinburgh, SA, 5111, Australia**	8. PERFORMING ORGANIZATION REPORT NUMBER
9. SPONSORING/MONITORING AGENCY NAME(S) AND ADDRESS(ES)	10. SPONSOR/MONITOR'S ACRONYM(S)
	11. SPONSOR/MONITOR'S REPORT NUMBER(S)

12. DISTRIBUTION/AVAILABILITY STATEMENT
Approved for public release, distribution unlimited

13. SUPPLEMENTARY NOTES
See also ADM001798, Proceedings of the International Conference on Radar (RADAR 2003) Held in Adelaide, Australia on 3-5 September 2003.

14. ABSTRACT

15. SUBJECT TERMS

16. SECURITY CLASSIFICATION OF:			17. LIMITATION OF ABSTRACT	18. NUMBER OF PAGES	19a. NAME OF RESPONSIBLE PERSON
a. REPORT	b. ABSTRACT	c. THIS PAGE			
unclassified	**unclassified**	**unclassified**	**UU**	**6**	

Standard Form 298 (Rev. 8-98)
Prescribed by ANSI Std Z39-18

II. Data Model

Let us define $\mathbf{x}(t)$ as the complex N-dimensional antenna array snapshot vector received at a particular range cell in a CPI composed of $t = 0, 1, \ldots, P-1$ pulses. In general, $\mathbf{x}(t)$ contains an additive mixture of radar clutter $\mathbf{c}(t)$, external interference $\mathbf{i}(t)$, internal noise $\mathbf{n}(t)$ and potentially a target signal $\mathbf{s}(t)$:

$$\mathbf{x}(t) = \mathbf{s}(t) + \mathbf{c}(t) + \mathbf{i}(t) + \mathbf{n}(t) \quad (1)$$

A far-field target echo received by a narrowband uniform linear array (ULA) can be expressed as $\mathbf{s}(t) = g(t)\mathbf{v}(\theta)$, where the scalar waveform $g(t)$ represents the target's temporal signature and $\mathbf{v}(\theta)$ is the spatial response (steering vector) for an angle-of-arrival θ that coincides with the radar look direction. An ideal target of constant reflectivity and radial velocity throughout the CPI has a signature $g(t) = \mu e^{j(2\pi f_d t + \phi)}$, where $\mu e^{j\phi}$ is the complex amplitude and f_d is the Doppler frequency shift normalised by the pulse repetition frequency (PRF). Under these conditions, the simplest target signal model may be defined as

$$\mathbf{s}(t) = \mu e^{j(2\pi f_d t + \phi)}[1, e^{j2\pi \frac{d}{\lambda}\sin\theta}, \ldots, e^{2\pi(N-1)\frac{d}{\lambda}\sin\theta}]^T \quad (2)$$

where d is the spacing between adjacent antenna elements, λ is the operating wavelength and $(\cdot)^T$ denotes transpose. The internal receiver noise is assumed to be uncorrelated with itself over different receivers and pulses. It is spatially and temporally white with the following correlation properties:

$$\mathbf{E}\{\mathbf{n}(r)\mathbf{n}^H(s)\} = \delta_{rs} \quad (3)$$

where σ_n^2 is the noise power, δ_{rs} is the Kronecker delta, $\mathbf{E}\{\cdot\}$ is the statistical expectation and H denotes the Hermitian transpose.

A. External Interference

Let $\mathbf{R}(t) = \mathrm{E}\{(\mathbf{i}(t) + \mathbf{n}(t))(\mathbf{i}(t) + \mathbf{n}(t))^H\}$ be the interference-plus-noise spatial covariance matrix at time t, the variation across different pulse repetition intervals (PRIs) arises only from the spatial non-stationarity of the external interference $\mathbf{i}(t)$, that is,

$$\mathbf{R}(t) = \mathbf{E}\{\mathbf{i}(t)\mathbf{i}^H(t)\} + \sigma_n^2\mathbf{I} \quad (4)$$

As $\mathbf{R}(t)$ is unknown in practice, it is often replaced by the sample spatial covariance matrix $\hat{\mathbf{R}}(t)$ estimated using secondary (clutter-free) snapshots $\mathbf{j}_k(t) = \mathbf{i}_k(t) + \mathbf{n}_k(t)$. Usually, secondary data is extracted from a *limited number* of K clutter-free range cells available at the t^{th} pulse. Using these snapshots, the sample estimate of the interference-plus-noise covariance matrix is given by

$$\hat{\mathbf{R}}(t) = \frac{1}{K}\sum_{k=1}^{K}\mathbf{j}_k(t)\mathbf{j}_k^H(t) \quad (5)$$

In a bistatic HFSW radar, secondary data may be extracted from range cells prior to the reception of the direct wave. In the monostatic case, the high attenuation of the surface wave with distance (more severe than the inverse square law) allows the clutter-free cells to be obtained at sufficiently long range. Otherwise the clutter must be pre-filtered [15], [16], [17].

If the CPI is partitioned into M sub-CPI or data batches containing Q pulses ($M = P/Q$), the adaptive beamforming weight vectors $\mathbf{w}_m$ for $m = 1, \ldots, M$ can be updated from batch-to-batch. Selection of batch length Q represents a compromise between fast updates to counteract interference non-stationarity and slow updates to increase secondary data sample support. Recall that the condition $KQ \geq 2N$ is required to provide satisfactory performance for the SMI technique [24]. The adaptive weights $\mathbf{w}_m$ are derived from the associated *integrated* sample covariance matrices $\mathbf{R}_m$,

$$\mathbf{R}_m = \frac{1}{Q}\sum_{t=Q(m-1)}^{Qm-1}\hat{\mathbf{R}}(t) \quad (6)$$

and applied to beamform the *test* range cell in the current batch: $y(t) = \mathbf{w}_m^H\mathbf{x}(t)$ for $t = Q(m-1), \ldots, Qm-1$. The similarity between the matrices $\mathbf{R}(t)$ being integrated depends on the batch length Q and the degree of interference spatial non-stationarity. In general, it is found that interference wavefronts reflected by the ionosphere fluctuate in a *correlated* manner with respect to time [9], [12]. In simple terms, this means that the matrices $\mathbf{R}(t)$ are likely to be similar over a number of adjacent PRI, but become progressively different as the structure of the interference wavefronts evolve in time (possibly varying appreciably in form between the endpoints of the CPI). A parametric interference model that quantifies this space-time behaviour was experimentally verified in [9], [13], [18], [19] using different data sets.

B. Surface Clutter

The dominant sea clutter contribution is produced by first-order scatter from specific spectral components of the ocean wavefield. These surface-height components are called Bragg waves. Their wavelength Λ is exactly half the radio wavelength λ and they move directly towards and away from the radar. In water of depth $h > \Lambda/2$, the Bragg wave trains move with radial velocity $v_g = \pm\sqrt{g\Lambda/2\pi}$, where $\Lambda = \lambda/2$ and g is acceleration due to gravity. This imposes a Doppler shift of $f_b = \pm\sqrt{g/\lambda\pi}$ on the first-order clutter backscattered at grazing incidence [20]. When the Bragg wave trains propagate through a surface current with mean radial velocity v_s, an additional Doppler shift $f_s = 2v_s/\lambda$ results for both the advance and recede Bragg wave spectral returns.

Let $r_i(t)$ be the first-order ocean clutter received at the *reference antenna element* in the array due to a scattering "patch" defined by the size of the (unnamed) test range cell and a *narrow-beam* at azimuth θ_i. In accordance with [21], this contribution to the total clutter return can be modelled in the time-domain as

$$r_i(t) = A_i e^{j\{2\pi(f_s+f_b)t+\phi_i(t)\}} + \tilde{A}_i e^{j\{2\pi(f_s-f_b)t+\phi_i(t)\}} \quad (7)$$

where A_i and $\tilde{A}_i$ are the advance and recede first-order clutter amplitudes respectively. These amplitudes are proportional to

the ocean directional wave-height spectrum at the Bragg wave-vectors (generally two orders of magnitude higher than the surrounding clutter continuum due to higher order scatter). As the primary concern is not to destroy the natural temporal coherence of the first-order clutter, we focus on modelling these dominant returns and omit the much weaker higher order scatter. In practice, the surface-current through the radar footprint may have a non-uniform velocity component with different dynamic behaviour from one scattering patch to another. Surface-current turbulence over the data collection period imposes a phase modulation $\phi_i(t)$ on the Bragg wave spectral components, a mechanism that broadens the approach and recede Bragg lines into identical shapes [22].

The overall first-order ocean clutter received at different antenna elements is the vector addition of the narrow-beam returns from I azimuth cells subtending the intersection of the transmit and receive beampatterns: $\mathbf{c}(t) = \sum_{i=1}^{I} r_i(t)\mathbf{v}(\theta_i)$. If a deterministic ground clutter component $\mathbf{c}_g$ with zero Hertz Doppler shift is also included, ignoring the movement of ground scatters and non-ideal systems effects, it follows that the clutter snapshots received by the array can be modelled as

$$\mathbf{c}(t) = \mathbf{c}_g + \mathbf{c}_a(t)e^{j2\pi(f_s+f_b)t} + \mathbf{c}_r(t)e^{j2\pi(f_s-f_b)t} \qquad (8)$$

where $\mathbf{c}_a(t) = \sum_{i=0}^{I} A_i e^{j2\pi\phi_i(t)}\mathbf{v}(\theta_i)$ is the modulation on the advance wave and $\mathbf{c}_r(t) = \sum_{i=0}^{I} \tilde{A}_i e^{j2\pi\phi_i(t)}\mathbf{v}(\theta_i)$ is that for the recede wave. The instantaneous Bragg frequencies change relatively slowly and may be regarded almost constant over a sufficiently short sub-CPI. The assumption of "frozen" Bragg frequencies over Q consecutive PRI allows the clutter to be represented as superposition of complex sinusoids with fixed frequencies over each sub-CPI. Such a model has previously been adopted to parametrically estimate surface currents [21] and to cancel clutter over CPI lengths shorter than 3 seconds [23].

In mathematical terms, we let $\mathbf{c}_a(t) = \mathbf{c}_a(\tau_m)e^{j2\pi\delta f_m t}$ and $\mathbf{c}_r(t) = \mathbf{c}_r(\tau_m)e^{j2\pi\delta f_m t}$ for $t = Q(m-1), \ldots, Qm-1$ where $\tau_m = Q(m-1)$ and δf_m is the slowly changing shift in Bragg wave instantaneous frequency that causes incoherent integration of the first-order ocean clutter over the CPI. By defining the matrix $\mathbf{A}_m = [\mathbf{c}_g, \mathbf{c}_a(\tau_m), \mathbf{c}_r(\tau_m)]$ and the vector $\mathbf{p}(t) = [1, e^{j2\pi(f_m+f_b)t}, e^{j2\pi(f_m-f_b)t}]^T$ for $f_m = f_s + \delta f_m$, the first order multi-channel clutter realisation is locally represented by a *dynamic spatial subspace* model with an instantaneous rank of $L = 3$ over each sub-CPI.

$$\mathbf{c}(t) = \mathbf{A}_m\mathbf{p}(t)\ , \quad t = Q(m-1), \ldots, Qm-1 \qquad (9)$$

In general, the minimum value of L is set by the number of dominant components resolved in the clutter Doppler spectra. For example, $L = 3$ corresponds to two resolved Bragg lines and ground clutter. Values of $L > 3$ may be adopted to account for subspace leakage caused by the continuous nature of the actual phase modulation process or to account for some of the second-order clutter. The condition $L \leq \text{Min}(Q, N)$ must be satisfied since Q snapshots of dimension N can be represented by a subspace of dimension less than or equal to $\text{Min}(Q, N)$.

III. Proposed Algorithm

The first adaptive beamformer $\mathbf{w}_1$ in the sequence is chosen to provide maximum SINR for the integrated sample covariance matrix $\mathbf{R}_1$ in accordance with the minimum variance distortionless response (MVDR) criterion. This weight vector is given by $\mathbf{w}_1 = [\mathbf{v}^H(\theta)\mathbf{R}_1^{-1}\mathbf{v}(\theta)]^{-1}\mathbf{R}_1^{-1}\mathbf{v}(\theta)$ and used to beamform the array snapshots $\mathbf{x}(t)$ received in the first batch at the test range cell; $y(t) = \mathbf{w}_1^H\mathbf{x}(t)$ for $t = 0, \ldots, Q-1$.

To avoid the coherence "discontinuity" across the batches without prohibiting the adaptive weight vector to change from batch-to-batch, the second weight vector $\mathbf{w}_2$ is formed in a manner that is *dependent* on the first $\mathbf{w}_1$ such that the instantaneous *change* in antenna pattern is constrained to be *orthogonal* to the clutter subspace in the second batch. Stated mathematically, the key idea of the proposed algorithm is to closely approximate the condition $(\mathbf{w}_2 - \mathbf{w}_1)^H\mathbf{A}_2 = \mathbf{0}$, as this permits $\mathbf{w}_2$ to change from $\mathbf{w}_1$ for interference rejection purposes while at the same time regulating this change such that it is not experienced by the clutter $\mathbf{c}(t) = \mathbf{A}_2\mathbf{p}(t)$ received in the second batch.

The clutter subspace in each batch is not observable because $\mathbf{x}(t)$ contains interference and noise. However, the adaptive filter $\mathbf{w}_1$ is still effective for interference removal in the first L pulses of the second batch. If necessary, this can be ensured by extending the covariance matrix estimate of $\mathbf{R}_1 = (Q+L)^{-1}\sum_{t=0}^{Q+L-1}\hat{\mathbf{R}}(t)$ to include the first L pulses of second batch. Applying this filter to the first L snapshots of the second batch yields $\mathbf{w}_1^H\mathbf{x}(t) \approx g(t) + \mathbf{w}_1^H\mathbf{c}(t)$ for $t = Q, \ldots, Q+L-1$, where the residual interference-plus-noise contribution at the beamformer output is assumed to be negligible compared with the unrejected clutter. Using the same argument, $\mathbf{w}_2^H\mathbf{x}(t) \approx g(t) + \mathbf{w}_2^H\mathbf{c}(t)$ for $t = Q, \ldots, Q+L-1$ since both weight vectors have unity gain response to the useful signal. If the second adaptive filter is made to satisfy L linear *data-driven* constraints defined by $\mathbf{w}_2^H\mathbf{x}(t) = \mathbf{w}_1^H\mathbf{x}(t)$ for $t = Q, \ldots, Q+L-1$, then to a good approximation, the clutter contribution at the output of the second filter is as if it were beamformed by the first filter (i.e. $\mathbf{w}_2^H\mathbf{c}(t) \approx \mathbf{w}_1^H\mathbf{c}(t)$ is approximated for $t = Q, \ldots, Q+L-1$) even though the two filters may be quite different ($\mathbf{w}_1 \neq \mathbf{w}_2$), as required for effective interference rejection.

As the L clutter snapshots $\mathbf{c}(t) = \mathbf{A}_2\mathbf{p}(t)$ at $t = Q, \ldots, Q+L-1$ are *linearly independent*, they collectively span the column space of the matrix $\mathbf{A}_2$. Consequently, the L data-driven constraints imposed on $\mathbf{w}_2$ encourage the relative change in antenna pattern to be orthogonal to the clutter subspace $(\mathbf{w}_2 - \mathbf{w}_1)^H\mathbf{A}_2 \approx \mathbf{0}$. This condition carries with it the implication that the clutter contribution at the output of the second filter is as if it were beamformed by the first filter over the *whole* of the second batch $t = Q, \ldots, 2Q-1$ despite the use of only L data-driven constraints. By defining $\mathbf{C}_2 = [\mathbf{v}(\theta), \mathbf{x}(Q), \ldots, \mathbf{x}(Q+L-1)]^H$ and $\mathbf{f}_2 = [1, \mathbf{x}^H(Q)\mathbf{w}_1, \ldots, \mathbf{x}^H(Q+L-1)\mathbf{w}_1]^T$ for the second batch, $\mathbf{w}_2$ is synthesised according to (10).

$$\min_{\mathbf{w}_2} \mathbf{w}_2^H\mathbf{R}_2\mathbf{w}_2 \qquad \text{subject to} \quad \mathbf{C}_2\mathbf{w}_2 = \mathbf{f}_2 \qquad (10)$$

This is the linearly constrained minimum variance (LCMV) optimisation problem which has the following solution [25].

$$\mathbf{w}_2 = \mathbf{R}_2^{-1}\mathbf{C}_2[\mathbf{C}_2^H\mathbf{R}_2^{-1}\mathbf{C}_2]^{-1}\mathbf{f}_2 \quad (11)$$

The remaining batches comprising the CPI are processed in similar fashion by iterating with respect to $m = 2, \ldots, M$ such that the mth weight vector $\mathbf{w}_m$ is computed as,

$$\mathbf{w}_m = \mathbf{R}_m^{-1}\mathbf{C}_m[\mathbf{C}_m^H\mathbf{R}_m^{-1}\mathbf{C}_m]^{-1}\mathbf{f}_m \quad (12)$$

for $\mathbf{C}_m = [\mathbf{v}(\theta), \mathbf{x}(Q(m-1)), \ldots, \mathbf{x}(Q(m-1)+L-1)]^H$ and $\mathbf{f}_m = [1, \mathbf{x}^H(Q(m-1))\mathbf{w}_{m-1}, \ldots, \mathbf{x}^H(Q(m-1)+L-1)\mathbf{w}_{m-1}]^T$. That is, the iterations are continued until the whole CPI is processed. Note that the proposed algorithm is *iterative* in the sense that the MVDR weight vector $\mathbf{w}_1$ initialises the sequence at $m = 1$ and the weights for batches $m = 2, \ldots, M$ are computed using the known weights from the *previous* step.

The adopted first-order clutter model allows the proposed algorithm to update the weight vector in non-overlapping batches whose length is primarily determined by the degree of interference spatial non-stationarity. This is different to the SC approach, where the adaptive filter is re-adjusted in "sliding window" fashion every PRI (irrespective of the interference characteristics) in an attempt to protect the AR clutter Doppler spectrum properties. The new philosophy not only provides robustness against the accumulation of weight vector estimation errors over the CPI, but also dramatically reduces the number of matrix inversions required and hence the computation load. For example, if $P = 256$, $L = 3$ and $M = 16$, the proposed method reduces the number of $N \times N$ sample covariance matrix inversions by a factor $F = \frac{P-L}{M} \approx 16$ which yields appreciable computational benefits for enabling real-time implementation.

IV. Experimental Results

Experimental data for this study was collected using the Iluka HFSW radar, located near Darwin in far north tropical Australia. The radar is bistatic with a high power (1-10 kW) transmit site at Stingray Head (65 km south-west of Darwin) and a lower power (100 W) site at Lee Point (10 km north-east of Darwin). The receiving system at Gunn Point (30 km North-East of Darwin) is based on a 500 m long ULA of 32 vertical monopoles, each antenna element is connected to a HF receiver and two dummy elements are added at either end of the array to reduce the effects of mutual coupling.

Each CPI is 32 seconds long and consists of $P = 256$ linear frequency modulated continuous waveform (FMCW) pulses or sweeps emitted with centre frequency $f_c = 7.719$ MHz, bandwidth $B = 50$ kHz and pulse repetition frequency (PRF) $f_p = 8$ Hz. The analysis is based on a ULA of $N = 20$ well-calibrated receivers, the full array could not be used because of some poor receivers that produced unreliable output. A total of 60 range cells were retained after receiver mixing and filtering, the first 12 clutter-free range cells providing the secondary snapshots for training the adaptive beamformers. The interference background was unknown and possibly arose due to a multiplicity of man-made and natural sources.

A. Conventional and SMI-MVDR Beamforming

Using $Q = 16$ PRI and $M = 16$ batches (i.e. update interval of 2 seconds), the SMI-MVDR beamformer was formed using $K = 10$ range cells per PRI ($KQ = 160 = 8N$) and applied to *clutter-free* range cell 12 to investigate interference rejection across ranges. Figure 1 compares the interference-plus-noise Doppler spectra processed by the conventional beamfomer (Hamming taper) and the time-varying SMI-MVDR adaptive beamformer with *no data-driven constraints*. Although both beamformers are normalised to unit gain in the look direction, the time-varying adaptive beamformer is seen to improve interference rejection by 15-20 dB across Doppler space.

Figure 2 shows the application of the same weights to beamform range cell 16 which additionally contains clutter and a real target (aircraft echo) in the vicinity of Doppler bin 38. Although the time-varying SMI-MVDR beamformer effectively rejects interference, it severely degrades target detection because the changing antenna patterns destroy the temporal coherence of the clutter (particularly the first-order returns) which smear across Doppler space and totally obscure the target echo.

B. Proposed Algorithm with Data-Driven Constraints

The same data was processed by the proposed adaptive beamformer using $L = 1, 2$ data-driven constraints. Figure 3 shows that $L = 1$ performs very poorly, a choice of $L = 2$ makes the target slightly more distinguishable but severely disturbs the clutter Doppler spectrum compared with the conventional beamformer output. It is evident from Figure 4 that the use of $L = 3$ data-driven constraints improves the SINR of a real target by approximately 20 dB relative to the conventional beamformer with no noticeable degradation in sub-clutter visibility. In other words, this time-sequence of adaptive weight vectors is felt by the interference but remains effectively "invisible" to the clutter.

Three ideal synthetic targets were injected in Doppler bins 53, 112 and 218 at test range cell 33 to compare the proposed adaptive beamformer with the steady-state or "fixed" SMI-MVDR beamformer trained on the same $K = 10$ range cells but over the whole CPI (i.e. $Q = 256$ PRI). Figure 5 shows that while both approaches can detect strong signals, either in the noise (bin 53) or near the clutter (bin 112), only the proposed method is capable of detecting the weaker high velocity target (bin 218).

C. Comparison with Stochastic Constraints Method

Figure 6 compares the performance of the proposed adaptive beamformer with $L = 3$ data-driven constraints against the SC method [14] based on a third order AR clutter model. The former is robust and produces sharper Bragg lines that enable a low velocity target near the right Bragg line (bin 112) to be detected. The large number of updates in the SC method results in a significant accumulation of estimation errors that not only widens the Bragg lines, but also smears clutter energy into other regions of Doppler space, making the weak high velocity target (bin 218) more difficult to detect.

Apart from the relative improvement in performance, the proposed adaptive beamfomer is about three times faster to compute than the SC method (timing tests run on an Alpha (DS20) 500 MHz computer). Hence, the proposed algorithm represents an attractive candidate for real-time implementation in practical HFSW radar systems.

V. Summary and Conclusion

This paper has presented a robust and computationally efficient adaptive beamforming algorithm for the cancellation of spatially non-stationary interference while preserving the Doppler spectrum characteristics of the dominant (first-order) clutter returns. The new method updates the weight vector at a rate determined the degree of interference non-stationarity, this is in contrast with the SC approach which re-adjusts the weight vector every PRI regardless of the interference characteristics in an attempt to protect the AR Doppler spectrum properties of the clutter (an update rate that is often faster than necessary for effective HF interference rejection).

Experimental results confirm that the proposed method can improve the SINR of real targets by 20 dB relative to the conventional beamformer in a HFSW radar. Apart from the computational advantage with respect to the SC technique, the proposed method was found to be more robust against the accumulation of estimation errors which degrade sub-clutter visibility. The benefits of the new approach with respect to previously existing methods have been demonstrated on a HFSW radar, although it is envisaged that the same technique can be applied to skywave OTH and other types of radar.

References

[1] S. Rotheram, "Ground wave propagation. I Theory for short distances", *Proceedings of the IEE, Part F: Communications, Radar and Signal Processing*, Vol. 128, No. 5, May 1981, pp 275-284.

[2] L. Sevgi, A. Ponsford and H. C. Chan, "An integrated maritime surveillance system based on high-frequency surface-wave radars, part 1: theoretical background and numerical simulations", *IEEE Antennas and Propagation Magazine*, Vol. 43, No. 5, October 2001, pp 28-43.

[3] A. Ponsford, L. Sevgi and H. C. Chan, "An integrated maritime surveillance system based on high-frequency surface-wave radars, part 2: operational status and system performance", *IEEE Antennas and Propagation Magazine*, Vol. 43, No. 5, October 2001, pp 52-63.

[4] S. J. Anderson, B. D. Bates and M. A. Tyler, "HF surface wave radar and its role in littoral warfare", *Journal of Battlefield Technology*, Vol. 2, No. 3, November 1999, pp 1-5.

[5] R. Dinger, E. Nelson, S. Anderson, F. Earl and M. Tyler, "High frequency radar cross section measurements of surrogate go-fast boats in Darwin, Australia", *Technical Report 1805, SPAWAR Systems Center*, San Diego, USA, September 1999.

[6] T. M. Blake, "The detection and tracking of small fast boats using HF surface wave radar", *HF Radio Systems and Techniques*, IEE Conference Publication No. 474, 2000, pp 219-224.

[7] X . L. Qiao and M. Jin, "Radio disturbance suppression for HF radar" *IEE Proc.- Radar, Sonar and Navigation*, Vol. 148, No. 2, April 2001, pp 89-93.

[8] H. W. Leong, "Adaptive suppression of skywave interference in HF surface wave radar using auxiliary horizontal dipole antennas", *Communications, Computers and Signal Processing*, IEEE Pacific Rim Conference, 1999, pp 128-132.

[9] G. A. Fabrizio, *Space-time characterisation and adaptive processing of ionospherically propagated HF signals*, Ph.D. dissertation, Adelaide University, July 2000, Australia.

[10] A. B. Gershman, U. Nickel and J. F. Bohme, "Adaptive beamforming algorithms with robustness against jammer motion", *IEEE Transactions on Signal Processing*, SP-45(7), July 1997, pp. 1878-1885.

[11] M. D. Turley and M. L. Lees, An adaptive impulsive noise suppressor for FMCW radar, *Digest 21st International Electronic Convention and Exhibition, IREECON*, Sydney, Australia, 1987.

[12] G. A. Fabrizio, Y. I. Abramovich, S. J. Anderson, D. A. Gray and M. D. Turley, "Adaptive cancellation of nonstationary interference in HF antenna arrays", *IEE Proceedings - Radar, Sonar and Navigation: Special Issue on Antenna Array Processing Techniques*, Vol. 145, No. 1, February 1998, pp. 19-26.

[13] G. A. Fabrizio, D. A. Gray and M. D. Turley, "Experimental evaluation of adaptive beamforming methods and interference models for high frequency over-the-horizon radar", *To appear in Multidimensional Systems and Signal Processing - Special Issue on Radar Signal Processing Techniques*. Vol. 14, No. 1-2, Jan-Feb 2003.

[14] Y. I. Abramovich, A. Y. Gorokhov, V. N. Mikhaylyukov and I. P. Malyavin, "Exterior noise adaptive rejection for OTH radar implementations", *ICASSP'94*, Adelaide, Australia, 1994, pp. 105-107.

[15] S. J. Anderson, Y. I. Abramovich and G. A. Fabrizio, "Stochastic constraints in nonstationary hot clutter cancellation", *In proceedings of ICASSP97*, Munich, Germany, pp 3753-3756.

[16] Y. I. Abramovich, N. Spencer and S. J. Anderson, "Stochastic constraints method in nonstationary hot clutter cancellation - part 1: Fundamentals and supervised training applications", *IEEE Transactions on Aerospace and Electronic Systems*, AES-34(4), 1998, pp. 1271-1292.

[17] Y. I. Abramovich, N. Spencer and S. J. Anderson, "Stochastic constraints method in nonstationary hot clutter cancellation - part 2: Unsupervised training applications", *IEEE Transactions on Aerospace and Electronic Systems*, AES-36(1), 2000, pp. 132-150.

[18] G. A. Fabrizio, D. A. Gray and M. D. Turley, "Parametric localisation of space-time distributed sources ", *In Proceedings of ICASSP 2000*, Istanbul, Turkey, June 2000, pp. 3097-3100.

[19] G. A. Fabrizio, D. A. Gray, M. D. Turley, and S. J. Anderson, "Modelling the spatial characteristics of ionospherically propagated HF signals", *In Proceedings of the International Radar Symposium (IRS)* , Munich, Germany, September 1998, pp. 1187-1197.

[20] B. J. Lipa and D. E. Barrick, "Extraction of sea-state from HF radar sea echo: mathematical theory and modeling", *Radio Science*, Vol. 21, No. 1, 1986, pp 81-100.

[21] K. Hickey, R. Khan and J Walsh, "Parametric estimation of ocean surface-currents with HF radar", *IEEE Journal of Ocean Engineeing*, Vol. 20, No. 2, April 1995, pp 139-144.

[22] M. L. Parkinson, "Observations of the broadening and coherence of MF/lower HF surface radar ocean echoes", *IEEE Journal of Ocean Engineeing*, Vol. 22, No. 2, April 1997, pp 347-363.

[23] B. Root, "HF radar ship detection through clutter cancellation", *IEEE National Radar Conference*, Dallas, May 1998, pp 281-286.

[24] I. S. Reed, J. D. Mallet and L. E. Brennan, "Rapid convergence rate in adaptive arrays", *IEEE Transactions on Aerospace and Electronic Systems*, AES-10(6), 1974, pp. 853-863.

[25] O.L. Frost, "An algorithm for linearly constrained adaptive array processing", *Proc. IEEE*, Vol.60, 1972, pp. 926-935.

VI. Acknowledgements

The authors acknowledge the Intelligence, Surveillance and Reconnaissance Division of the Defence Science and Technology Organisation, Australia, and the Iluka operators. In particular Dr Bruce Ward, Mr Paul Amey and Mr Mark Tyler are gratefully acknowledged for supporting this work and making the experimental data available. The first author also thanks Prof Yuri Abramovich and Prof Stuart Anderson for a number of useful discussions on the subject of this paper.

The work of the second author was supported in parts by the Natural Sciences and Engineering Research Council (NSERC) of Canada, Communications and Information Technology Ontario (CITO), Premier Research Excellence Award Program of the Ministry of Energy, Science, and Technology (MEST) of Ontario, and Wolfgang Paul Award Program of the Alexander von Humboldt Foundation.

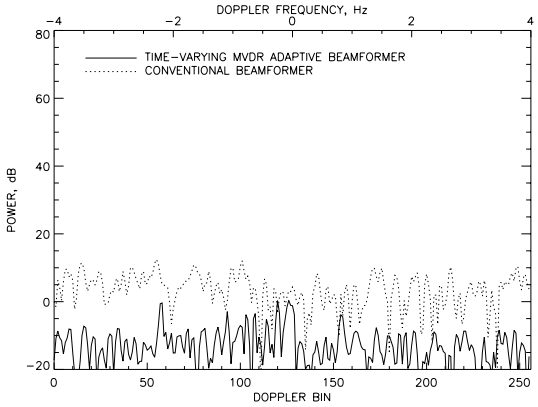

Fig. 1. Interference-plus-noise Doppler spectra for conventional (Hamming taper) beamformer and time-varying MVDR adaptive beamformer with *no data-driven constraints*.

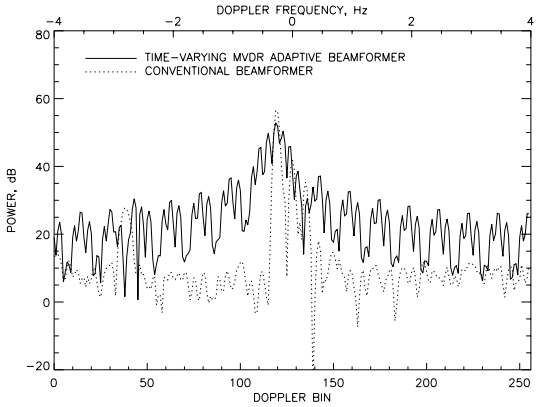

Fig. 2. Operational radar Doppler spectra for the conventional (Hamming taper) beamformer and time-varying MVDR adaptive beamformer with *no data-driven constraints*.

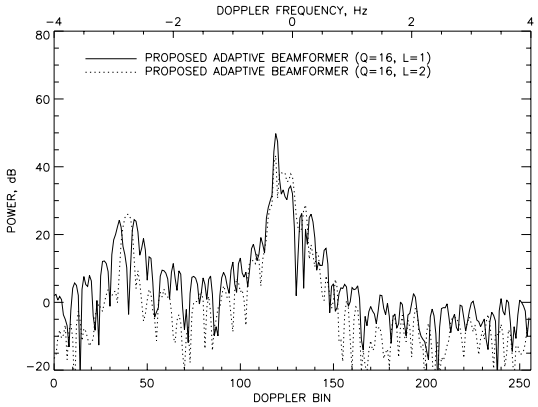

Fig. 3. Operational radar Doppler spectra for the proposed adaptive beamformer with $L = 1$ and $L = 2$ data-driven constraints.

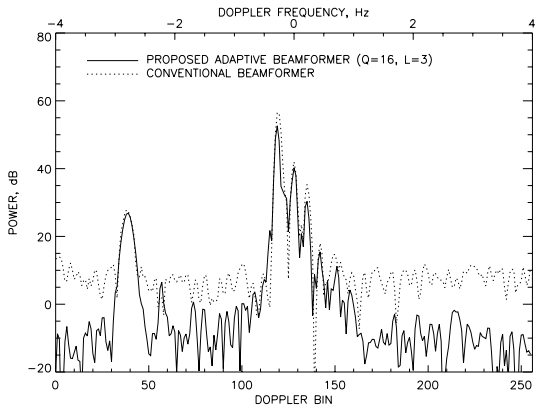

Fig. 4. Operational radar Doppler spectra for the conventional (Hamming taper) beamformer and proposed adaptive beamformer with $L = 3$ data-driven constraints.

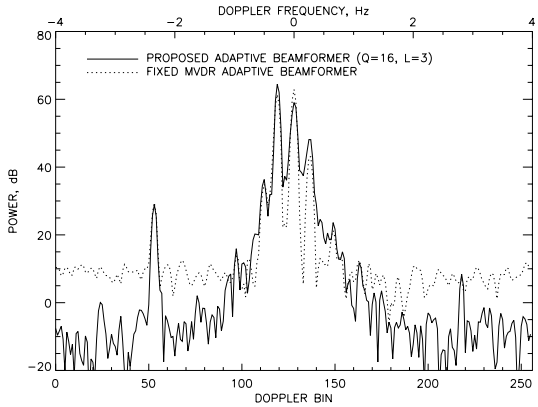

Fig. 5. Operational radar Doppler spectra with synthetically injected targets for the *fixed* MVDR and proposed adaptive beamformers.

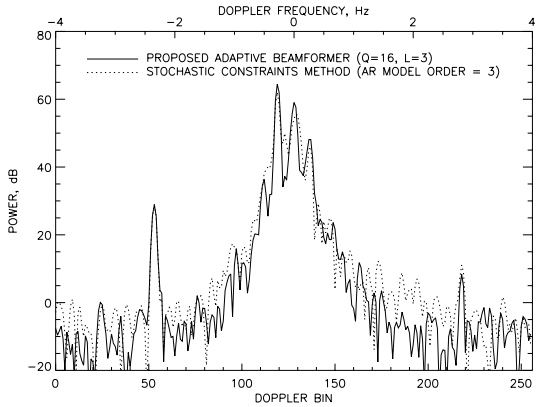

Fig. 6. Operational radar Doppler spectra with synthetically injected targets for the stochastic constraints and proposed adaptive beamformers.